



New generation of supramolecular mixtures: Characterization and solubilization studies

Tracy El Achkar, Leila Moura, Tarek Moufawad, Steven Ruellan, Somenath Panda,
Stéphane Longuemart, François-Xavier Legrand, Margarida Costa Gomes, David
Landy, Hélène Greige-Gerges, et al.

► **To cite this version:**

Tracy El Achkar, Leila Moura, Tarek Moufawad, Steven Ruellan, Somenath Panda, et al.. New generation of supramolecular mixtures: Characterization and solubilization studies. *International Journal of Pharmaceutics*, 2020, Part of special issue Special Issue in Honor of Professor Thorsteinn Loftsson on the Occasion of His 70th Birthday, 584, pp.119443. [10.1016/j.ijpharm.2020.119443](https://doi.org/10.1016/j.ijpharm.2020.119443). [hal-03102809](https://hal.archives-ouvertes.fr/hal-03102809)

HAL Id: hal-03102809

<https://hal.science/hal-03102809v1>

Submitted on 22 Aug 2022

HAL is a multi-disciplinary open access archive for the deposit and dissemination of scientific research documents, whether they are published or not. The documents may come from teaching and research institutions in France or abroad, or from public or private research centers.

L'archive ouverte pluridisciplinaire **HAL**, est destinée au dépôt et à la diffusion de documents scientifiques de niveau recherche, publiés ou non, émanant des établissements d'enseignement et de recherche français ou étrangers, des laboratoires publics ou privés.



Distributed under a Creative Commons CC BY-NC 4.0 - Attribution - Non-commercial use - International License

New generation of supramolecular mixtures: characterization and solubilization studies

Tracy El Achkar^{a,b}, Leila Moura^a, Tarek Moufawad^{a,c}, Steven Ruellan^a, Somenath Panda^a, Stéphane Longuemart^d, François-Xavier Legrand^e, Margarida Costa Gomes^c, David Landy^a, Hélène Greige-Gerges^b, Sophie Fourmentin^{a,*}

^aUnité de Chimie Environnementale et Interactions sur le Vivant (UCEIV, UR 4492), SFR Condorcet FR CNRS 3417, Université du Littoral Côte d'Opale, 59140 Dunkerque, France

^bBioactive Molecules Research Laboratory, Faculty of Sciences, Lebanese University, 1202 Jdeidet El Metn, Lebanon

^cLaboratoire de Chimie, ENS Lyon, UMR CNRS 5182, 46 Allée Italie, 69007 Lyon, France

^dUnité Dynamique et Structures des Matériaux Moléculaires (UDSMM, EA 4476), Université du Littoral Côte d'Opale, 59140 Dunkerque, France

^eInstitut Galien Paris-Sud, Université Paris-Sud, CNRS, Université Paris-Saclay, 92290 Châtenay-Malabry, France

*Corresponding author: lamotte@univ-littoral.fr

Abstract

In this work, a series of novel low melting mixtures (LMM) based on cyclodextrins (CD) and levulinic acid and inspired by the deep eutectic solvents (DES), were prepared. These supramolecular mixtures are the first reported CD-based mixtures that are liquid at room temperature. Density, viscosity and rheological measurements as well as differential scanning calorimetry and thermogravimetric analysis were performed to characterize these new LMM. Nuclear magnetic resonance (NMR) spectroscopy was used to monitor their stability. Furthermore, their ability to solubilize *trans*-anethole (AN) and related essentials oils were evaluated by static headspace-gas chromatography (SH-GC), in comparison with water. AN was up to 1300 times more soluble in the CD-based LMM than in water. Finally, multiple headspace extraction (MHE) was used to monitor the release of AN from these LMM. After 10 extractions, 20 to 40% of AN was released from the studied LMM, while 70% was released from water. The new CD-based LMM have potential applications for solubilization and delivery of poorly soluble drugs.

Keywords: cyclodextrins, static headspace-gas chromatography, *trans*-anethole, essential oils, low melting mixtures.

1. Introduction

Cyclodextrins (CD) are non-toxic cyclic oligosaccharides obtained from the enzymatic degradation of starch (Crini, 2014; Szejtli, 1998). Native CD, which are produced at an industrial scale, consist of six (α -CD), seven (β -CD) or eight (γ -CD) α -(1 \rightarrow 4) linked D-glucopyranose units. Due to their hydrophobic internal cavity and hydrophilic external surface, these water-soluble molecules have been extensively used to encapsulate hydrophobic and volatile compounds by forming host-guest inclusion complexes (Ciobanu et al., 2013; Kfoury et al., 2019, 2015; Marques, 2010).

β -CD is the most studied and most frequently used CD, because of its cheapness and availability. However, it is the least water-soluble of the three native CD. Therefore, various β -CD derivatives have been synthesized and are commercially available. CD and their derivatives have attracted interest for a wide range of applications such as food, agrochemistry, environmental chemistry, catalysis, cosmetics and pharmaceuticals (Crini et al., 2018; Kurkov and Loftsson, 2013; Landy et al., 2012; Legrand et al., 2009; Loftsson and Masson, 2001; Nguyễn et al., 2017; Potier et al., 2012).

The discovery of deep eutectic solvents (DES) in 2003 was a turning point in the world of green chemistry (Abbott et al., 2003). Since then the publications in this field have increased exponentially. Being easy to prepare from cheap and widely available starting materials, DES have attracted a lot of attention from researchers in the past few years and have found applications in a wide range of domains: metal processing, synthesis, electrochemistry, solubilization of gas and pollutants, extraction of bioactive compounds and as drug solubilization vehicles (El Achkar et al., 2019; Li and Lee, 2016; Mbous et al., 2017; Morrison et al., 2009; Moura et al., 2017; Zhang et al., 2012). These solvents

are obtained by mixing two or three compounds that are able to associate, mainly by the formation of hydrogen bonds, at a particular molar ratio to form a clear homogenous liquid with a lower melting point than that of the individual components (Zhang et al., 2012). Among them, DES based on carbohydrates and other primary metabolites have been described lately (Choi et al., 2011). These DES are called natural deep eutectic solvents (NADES). In this respect, cyclodextrins (CD) are potential NADES-forming compounds.

Only a few studies have investigated the combined use of CD and DES. Some studies have evaluated the possibility of forming low melting mixtures (LMM) with CD and *N,N'*-dimethylurea (DMU) (Ferreira et al., 2015; Imperato et al., 2005; Jérôme et al., 2014). A LMM was indeed obtained with various CD derivatives. Hydroformylation, Tsuji-Trost and Diels–Alder reactions were efficiently performed in these new solvents with high catalytic activity. However, the melting point of these LMM was superior to 80 °C, limiting their scope of application. Thereafter, we have patented the use of DES for the absorption of volatile organic compounds (VOC) and described the beneficial effect of adding CD on VOC solubility in a choline chloride:urea (ChCl:U) DES (Fourmentin et al., 2016). At the same time, a study showing that the solubility of the three native CD was remarkably enhanced in the same DES was published (McCune et al., 2017). Moreover, it was recently reported that no aggregation of β -CD occurred in ChCl:U up to concentrations of 800 mg/mL (Triolo et al., 2020). Methyl- β -CD has also been incorporated into aqueous solutions of a DES based on glycerol and glycine and described to improve the extraction of polyphenols (Athanasiadis et al., 2018). Later, we investigated the advantage of combining ChCl:U and CD to solubilize various volatile

compounds and demonstrated that CD maintain their host-guest properties in CHCl_3 :U (Di Pietro et al., 2019; Dugoni et al., 2019; Moufawad et al., 2019). Combinations of DES and CD can potentially give rise to highly attractive materials; however, having a solvent based on CD could be even more useful. To this end, we recently reported the first supramolecular mixture based on randomly methylated- β -CD (RAMEB) and levulinic acid and showed that RAMEB retained its inclusion properties (El Achkar et al., 2020).

In the present study, three new supramolecular mixtures were prepared using new β -CD derivatives (HP- β -CD, CRYSMEB and Captisol®) in addition to RAMEB as hydrogen bond acceptors (HBA) with levulinic acid (Lev) as hydrogen bond donor (HBD) (Figure 1). Density, viscosity and rheological measurements, differential scanning calorimetry and thermal gravimetric analysis were carried out to characterize these new liquid mixtures. Moreover, their stability was evaluated as a function of time and temperature by NMR. Finally, their ability to solubilize trans-anethole (AN), star anise and fennel essential oils was evaluated by static headspace-gas chromatography (SH-GC) and multiple headspace extraction (MHE) was used to monitor the release of AN from these mixtures.

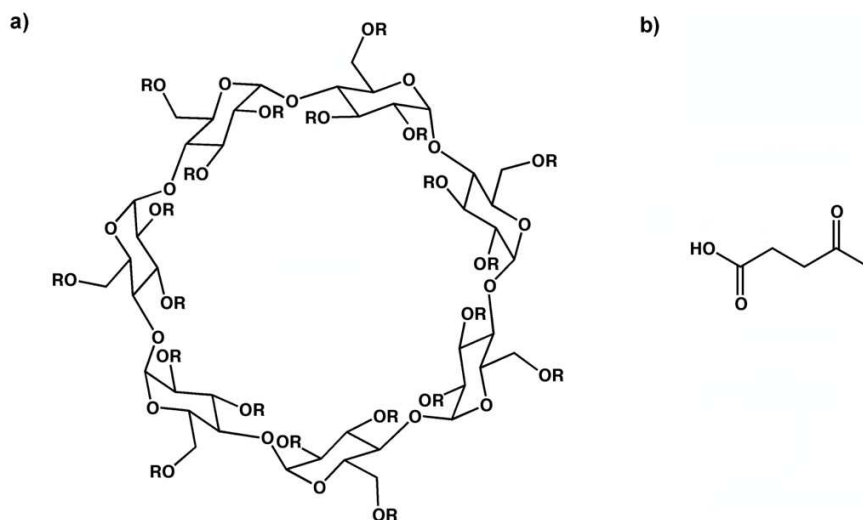


Figure 1. Structures of the low melting mixtures constituents a) General structure of β -cyclodextrin derivatives: HP- β -CD (degree of substitution (DS) = 5.6), R= -H or -CH₂-CH(OH)-CH₃; RAMEB (DS = 12.9), R= -H or -CH₃; CRYSMEB (DS = 4.9), R= -H or -CH₃; Captisol® (DS = 6.5), R= -H or -(CH₂)₄-SO₃⁻ Na⁺; b) Levulinic acid.

2. Experimental Section

2.1. Materials

trans-Anethole [1-methoxy-4-(1-propenyl)-benzene] (99%) was purchased from Acros Organics, France. Levulinic acid (98%) was purchased from Sigma-Aldrich, France. Randomly methylated- β -CD (RAMEB, DS =12.9), low methylated- β -CD (CRYSMEB, DS = 4.9) and hydroxypropyl- β -CD (HPBCD, DS= 5.6) were provided by Roquette Frères (Lestrem, France). Sulfobutylether- β -CD (Captisol®, DS= 6.5) was provided by LIGAND Pharmaceuticals (San Diego, CA, USA). All compounds were used as received.

Essential oils of *Illicium verum* (star anise) and *Foeniculum vulgare* (fennel) were provided by Herbes et Traditions (Comines, France). The main constituents (>1%) of

the essential oils are: *trans*-anethole (91.07%) and limonene (3.28%) for star anise; *trans*-anethole (75.30%), estragole (3.10%) and fenchone (2.10%) for fennel (data provided by Herbes et Traditions).

2.2. Preparation of the supramolecular mixtures

The LMM were prepared by mixing the HBA and the HBD at a fixed molar ratio (Table 1). The mixtures were then stirred at 60 °C until the formation of a clear homogenous liquid then cooled at room temperature. All the prepared mixtures were liquid at room temperature. As CD possess a large number of HBA sites (35 sites for the native β -CD and 35 to 55 sites for the modified β -CD), we used a large molar excess of levulinic acid. The water content of all the prepared mixtures was determined using Karl Fisher titration method (Mettler Toledo DL31) and was found to vary between 2.5 and 3.9 wt.% (Table 1).

Table 1. Composition and water content of the prepared LLM.

CD:Lev mixture	HBA	HBD	HBA:HBD molar ratio	Water content (wt. %)
HPBCD:Lev	Hydroxypropyl- β -CD	Levulinic Acid	1:32	2.7
RAMEB:Lev	Randomly methylated β -CD		1:27	2.5
CRYSMEB:Lev	Low methylated β -CD		1:25	3.3
Captisol®:Lev	Sulfobutylether- β -CD		1:44	3.9

We should point out that our attempts to obtain liquid mixtures with the three native CDs failed, which tends to emphasize that the density and flexibility of the hydrogen bond network are probably key parameters for the formation of liquid mixtures. It seems that

the breakdown of hydrogen bonds from one glucose to another within CD molecules could be a prerequisite, therefore limiting the preparation of such LMM to modified CDs.

2.3. Stability studies of LMM by NMR

In order to evaluate whether any esterification reaction occurred between the remaining hydroxyl groups of the CD derivatives and levulinic acid, the supramolecular mixtures were prepared at 30 °C and were subjected to gradual heating. Aliquots were withdrawn at different times and temperatures, then diluted with DMSO-*d*₆, or CDCl₃, in the case of Captisol®:Lev, and analyzed by NMR. The first aliquot of the mixture was taken when a clear liquid was formed (*t*₀). The other aliquots were withdrawn at 30, 60, 80 and 100 °C. The mixtures were kept for 24 hours at the desired temperature prior to analysis. ¹³C NMR experiments were recorded on a Bruker Avance III spectrometer operating at 400 MHz for the proton nucleus, equipped with a multinuclear z-gradient BBFO probe head. The probe temperature was maintained at 30 °C and standard 5 mm NMR tubes were used. ¹³C spectra were recorded with the following acquisition parameters: time domain 65 K with a digital resolution of 0.73 Hz, relaxation delay: 2 s and 1536 scans.

2.4. Density and viscosity measurements

Density measurements were carried out using a U-shaped vibrating-tube densimeter (Anton Paar, model DMA 5000 M) operating in a static mode. The factory calibration was used and verified before and after each measurement with air and tri-distilled degassed water. The DMA 5000 densimeter performs an analysis with an estimated uncertainty in density and temperature of ± 0.1 kg m⁻³ and ± 0.001 °C, respectively.

The viscosity was determined using a falling-ball-based microviscosimeter (Lovis 2000 M/ME from Anton Paar). The temperature was controlled to within 0.005 °C and measured with an accuracy better than 0.02 °C. A capillary tube of 1.8 mm diameter, previously calibrated as a function of temperature and angle of measurement with reference oils, was used for the measurements. The overall uncertainty on the viscosity was estimated to be 2%. All measurements were performed at atmospheric pressure and at temperatures ranging between 30 and 60 °C, as previously described (Moufawad et al., 2019).

2.5. Rheological measurements

Rheological measurements were performed with an AR-G2 controlled-stress rotational rheometer (TA Instruments). Flow curves were obtained with an aluminum cone-plate geometry (40 mm diameter, 1° cone angle, 28 µm truncation gap). A three-step shear rate sweep was imposed after a 3-minute equilibration time: 1) increase of the shear rate from 0.1 to 5000 s⁻¹ over 3 min (upwards curve), 2) peak hold at 5000 s⁻¹ during 1 min, 3) decrease of the shear rate from 5000 to 0.1 s⁻¹ over 3 min (downwards curve). The temperature was maintained at 30 °C and controlled with a Peltier plate. Measurements were performed in triplicate at least for each sample, to ensure reproducibility. The statistical analysis was performed by calculating the standard deviation from the three measurements or more made for each sample.

2.6. Differential scanning calorimetry (DSC)

DSC experiments were carried out using a Q1000 DSC (TA Instruments) with a temperature range from -100 °C to 40 °C and at a thermal scanning rate of 5 °C.min⁻¹. All the samples (HPBCD:Lev, RAMEB:Lev, CRYSMEB:Lev and Captisol®:Lev) were encapsulated in aluminum pans (sample weight ~ 10-15 mg), sealed with hermetic lids and analyzed. Experiments were performed under nitrogen flow (50 mL.min⁻¹).

2.7. Thermal gravimetric analysis (TGA)

TG measurements were performed with a TGA550 thermogravimetric analyzer (TA Instruments). Samples were placed in an open platinum pan (100 µL) suspended in the furnace. The initial weight of the sample was around 25-30 mg, and nitrogen was used as the purge gas at a fixed flow of 20 mL.min⁻¹. The weight of material was recorded during heating from room temperature to 600 °C at a heating rate of 10 °C.min⁻¹.

2.8. Static Headspace-Gas Chromatography (SH-GC)

AN, star anise and fennel essential oils (EO) were added to water or to the LMM placed in 22 mL headspace glass vials. Vials were then sealed and thermostated at 30 °C under stirring for 24 hours in order to reach equilibrium between liquid and gaseous phases. Subsequently, 1 mL of the gaseous phase was withdrawn from the vial and injected in the chromatographic column for analysis via a heated transfer line.

All experiments were carried out with an Agilent G1888 headspace sampler coupled with a Perkin Elmer Autosystem XL gas chromatography equipped with a flame ionization detector and a DB624 column using nitrogen as carrier gas. The GC column temperature was fixed at 160 °C for AN. For the analysis of EO, temperature conditions

were set as follows: initial temperature of 50 °C for 2 min, increased to 200 °C at 5 °C.min⁻¹, then hold for 2 min, giving a total runtime of 34 min.

2.8.1. Determination of partition coefficient (*K*)

The vapor-liquid partition coefficient (*K*) is the ratio of the concentration of a substance in vapor phase to its concentration in liquid phase, when the equilibrium is reached (Kolb and Ettre, 2006).

$$K = \frac{C_G}{C_L} \quad (1)$$

K of AN was determined in water and in the different supramolecular mixtures at 30 °C by using the phase ratio variation method for AN in water and the vapor phase calibration method for AN in the supramolecular mixtures as reported earlier (Moura et al., 2017).

2.8.2. Retention of AN and essential oils (EO)

The retention of AN, star anise and fennel EO in the formulations was estimated according to procedures developed for aromas (Decock et al., 2008) and EO (Kfoury et al., 2015), respectively. The percentage of retention of AN and EO by the LMM was determined by SH-GC at 30 °C following equation (2) for AN and equation (3) for EO:

$$\% \text{ Retention} = \left(1 - \frac{A_{LMM}}{A_W}\right) \times 100 \quad (2)$$

where A_{LMM} and A_W stand for the peak area of AN in presence of LMM and of water, respectively.

$$\% \text{ Retention} = \left(1 - \frac{\Sigma A_{LMM}}{\Sigma A_W} \right) \times 100 \quad (3)$$

where ΣA_{LMM} and ΣA_W stand for the sum of peak areas of the EO components in presence of LMM and of water, respectively.

2.8.3. Multiple Headspace Extraction (MHE)

MHE is a quantitative method, consisting of successive headspace extractions (Kolb and Ettre, 2006). It was used to study the release kinetics of AN from the prepared LMM at 60 °C. Samples were prepared similarly to the previous experiments but, once equilibrium was reached, vials were subjected to 10 headspace extractions at 1-hour intervals.

3. Results and Discussion

3.1. Stability studies of LMM by NMR

A recent study showed that ChCl:carboxylic acid DES underwent esterification regardless of the method or the temperature employed during their preparation. However, the DES based on levulinic acid was the least affected, with only 6 mol% of the ChCl esterified at 100 °C (Rodriguez Rodriguez et al., 2019). In the present study,

the thermal stability of the new supramolecular mixtures was investigated using ^{13}C NMR, by following the modification of the chemical shift of the carboxylic acid function of levulinic acid. All the supramolecular mixtures were stable after consecutive exposures of 24 hours at 30 and 60 °C. After an additional 24 hours at 80 °C, a small amount of esterification was observed and identified by the presence of a new broad signal around 173.0 ppm corresponding to the ester function (Figure S1). No esterification was detected in the case of Captisol®:Lev, which could be due to steric hindrance from the relatively bulky sulfobutyl ether moieties. On the other hand, the most affected LMM was HPBCD:Lev with the relative intensity ratio of the esterified carbon peak being 1.6% of the carboxylic acid carbon peak at 100 °C (Table S1) and could be the result of a higher reactivity of the hydroxyl groups, especially that of the hydroxypropyl moieties. Therefore, the preparation of the LMM was performed at 60 °C for all other experiments, in order to avoid esterification. Furthermore, the long-term stability of the LMM was evaluated after 18 months of storage at room temperature. The mixtures showed no degradation over time. The low esterification ratio observed for these CD-based mixtures compared with ChCl-based DES could be explained by the fact that the remaining hydroxyl groups of the CD derivatives used in this study are sterically hindered since the degree of substitution varied from 4.9 to 12.9.

3.2. Physicochemical characterization

The density and viscosity values of the four LMM (HPBCD:Lev, RAMEB:Lev, CRYSMEB:Lev and Captisol®:Lev) were measured from 30 to 60 °C, at 10 °C intervals (Figure 2 and Tables S2 and S3). CD-based mixtures presented higher density values

(ranging between 1184.5 and 1234.3 kg m⁻³ at 30 °C) compared with common DES based on levulinic acid (1134.5 and 1105.7 kg m⁻³ at 303.15 K for ChCl:Lev or TBPBr:Lev DES respectively) (Moufawad et al., 2019; Moura et al., 2017). Additionally, the obtained values fall in the 1000-1300 kg m⁻³ range of density values observed with most of the reported DES (Tang and Row, 2013). LMM were also more viscous than these common DES, except for RAMEB:Lev which presents similar viscosity to ChCl:Lev (212.9 and 206.2 mPa.s at 30 °C, respectively).

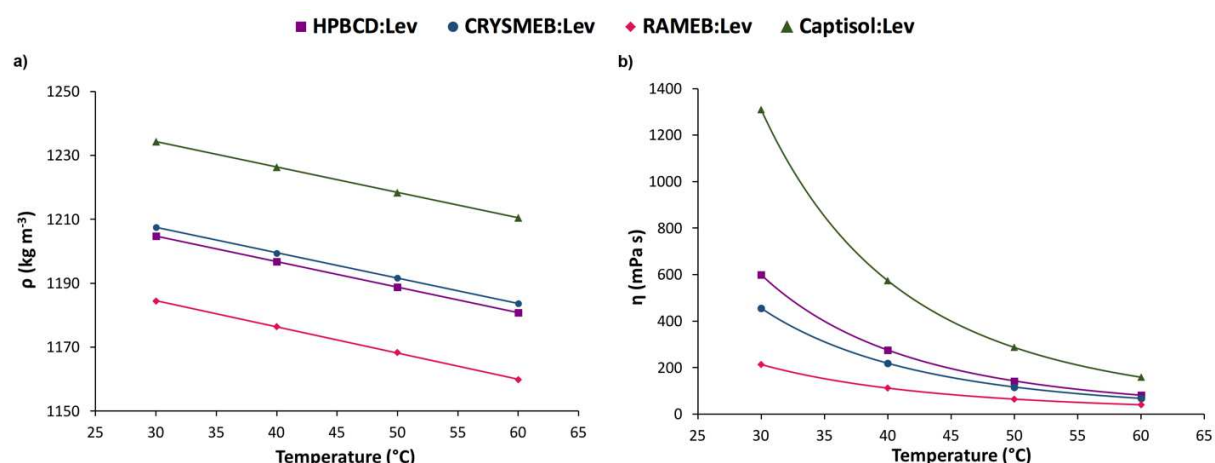


Figure 2. Experimental values of the density (a) and viscosity (b) of the supramolecular LMM. The lines represent the Vogel–Fulcher–Tammann (VFT) correlation fitting for viscosity and appropriate polynomials in the case of the density.

Nevertheless, the viscosity values decreased remarkably with increasing temperature. All CD-based mixtures, except Captisol®:Lev, show relatively low viscosities (≤ 80 mPa.s) at 60 °C. The relatively higher viscosity of Captisol®:Lev can be explained by a stronger hydrogen bond network, given the higher number of HBA sites present in Captisol® compared to the other studied β -CD derivatives due to the presence of the

sulfonate groups. In addition, the CD:Lev mixtures were less viscous than the mixtures based on β -CD derivatives and *N,N'*-dimethylurea. Indeed, the latter mixtures present a melting point above 80 °C and their viscosities were at least equal to 205.0 mPa.s at 90 °C (Jérôme et al., 2014).

The flow behavior of the four LMM was then investigated at 30 °C. All the mixtures studied exhibit a Newtonian plateau for shear rates below 1000 s⁻¹ and shear-thinning behavior for shear rates above this value (Figure S2). The measured static and dynamic viscosities for the same composition were slightly different (for example, in the case of RAMEB:Lev at 30 °C, $\eta_{\text{static}} = 212.9$ mPa.s vs. $\eta_{\text{dynamic}} = 245.0$ mPa.s) but the same order was found for the viscosities ($\eta_{\text{Captisol@:Lev}} > \eta_{\text{HPBCD:Lev}} > \eta_{\text{CRYSMEB:Lev}} > \eta_{\text{RAMEB:Lev}}$). Moreover, the shear-thinning behavior was more pronounced as the viscosity increased. Indeed, for a high shear rate of 5000 s⁻¹, a decrease of around 29% in viscosity was observed for Captisol@:Lev, whereas in the case of RAMEB:Lev a smaller decrease (around 8%) was detected. As explained above, the most viscous mixtures probably contain a larger number of hydrogen bonds that may be disrupted at high shear rates, leading to a greater decrease in viscosity.

3.3. Thermal properties

DSC measurements were performed over a range of -100 to 40 °C in order to understand the thermal events occurring in this temperature range. We chose to focus on the lower temperature range, given that the samples under study were all liquid at room temperature. Interestingly, none of the CD-based mixtures, *i.e.* HPBCD:Lev, RAMEB:Lev, CRYSMEB:Lev and Captisol@:Lev, showed any melting point in the

heating curve. Instead, glass transition curves with T_g at -73.3, -74.3, -73.5 and -67.8 °C were observed respectively for the mixtures (Figure 3a). This absence of melting peaks and presence of glass transition temperature was widely observed in the literature. For example, Francisco et al. reported 21 systems showing no melting point but glass transition temperatures ranging between -13.64 and -77.73 °C (Francisco et al., 2012) while Dai et al. identified 13 different NADES with $T_g < -50$ °C and no melting point (Dai et al., 2013). Likewise, with the exception of glass transition, no other thermal events occur for trehalose:glycerol at a 1:30 molar ratio (Castro et al., 2018). Moreover, the observed T_g value of -75.14 °C is interestingly pretty close to the values obtained for our CD-based mixtures. CD generally present a T_g ranging between 80 °C and more than 200°C depending on the CD (Tabary et al., 2011). Therefore, the observed T_g values could be attributed to the formation of a LMM with levulinic acid.

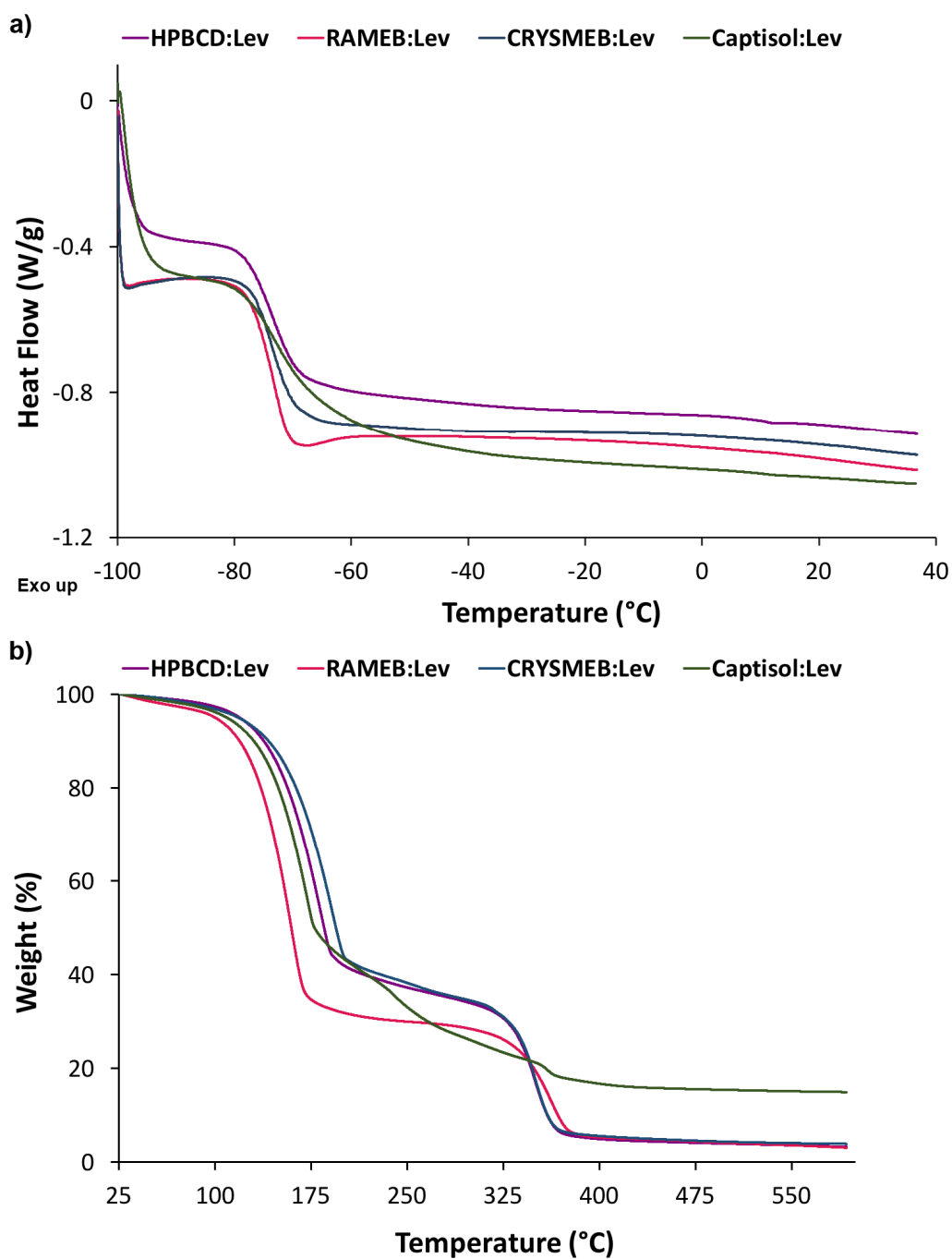


Figure 3. DSC (a) and thermogravimetric analysis (b) curves of the LMM.

Dynamic thermogravimetric analysis (TGA) was used to further investigate the thermal stability of the new mixtures. As shown in Figure 3b, they underwent progressive

decomposition as the temperature increased. Their decomposition showed a two-step weight loss similar to choline-based DES (Delgado-Mellado et al., 2018). At around 130 °C, levulinic acid began to decompose while the CD began to degrade at about 325 °C, except in the case of Captisol® for which the second decomposition began at around 225 °C and a third decomposition was determined near 350 °C. From the thermogravimetric curve in Figure 3b, the results showed that the thermal decomposition temperatures corresponding to the first thermal event of HPBCD:Lev, RAMEB:Lev, CRYSMEB:Lev and Captisol®:Lev were equal to 130.4, 117.6, 137.7 and 127.6 °C respectively. CRYSMEB:Lev had the best thermal stability and RAMEB:Lev the worst (Table S3). The DSC and TGA results demonstrate that these CD-based mixtures retain a stable liquid state over a wide temperature range.

3.4. Solubilization of AN and essential oils

AN has incited interest from the food, cosmetics and pharmaceutical industries due to its attractive properties. In fact, AN is a major component of star anise and fennel essential oils which are known both as flavoring agents and as medicines owing to their numerous biological properties (Auezova et al., 2020; Diao et al., 2014; Wang et al., 2018). However, its wider applications are hampered by drawbacks related to its high volatility, low water solubility and chemical instability. We have previously investigated the effect of AN complexation with various CD on its solubility and photodegradation and showed that CD were able to improve AN solubility and stability through inclusion complex formation (Kfoury et al., 2014a, 2014b). Therefore, the ability of the LMM to solubilize AN was evaluated by determining the vapor-liquid partition coefficient K of AN

(Table 2) as well as the percentage of AN retention. More than 99% of AN were retained by all the studied mixtures while in aqueous solution CD were able to reduce AN volatility only up to 92% leading to around 20-fold reduction in K (Kfoury et al., 2014b, 2014a). In the case of the supramolecular mixtures we observed up to 1300 times reduction in K compared with water (Table 2).

Table 2. Partition coefficient (K) values of *trans*-anethole in water and in the tested mixtures and ratio of $K_{\text{water}}/K_{\text{LMM}}$ at 30°C

	K	Ratio
Water	1.29×10^{-2}	1
HPBCD:Lev	1.04×10^{-5}	1240
RAMEB:Lev	9.60×10^{-6}	1343
CRYSMEB:Lev	1.08×10^{-5}	1194
Captisol®:Lev	2.18×10^{-5}	592

DES have been explored as solvents for the extraction of EO or their components in the past few years (Li et al., 2019; Ozturk et al., 2018), with higher extraction yields observed compared with conventional solvents. However, the majority of the reported studies used diluted DES to improve their extraction efficiency by reducing their viscosity or increasing their polarity (Jeong et al., 2018). To the best of our knowledge, no studies investigating the solubilization or the extraction of AN or star anise EO using DES have been performed to date. Only one publication has reported the use of lactic acid-based NADES for the extraction of polyphenols from fennel EO, among other

Greek medicinal plants (Bakirtzi et al., 2016). Subsequently, the ability of the studied LMM to solubilize EO, as well as AN in the presence of other aroma compounds, in two EO was investigated.

Star anise and fennel EO were chosen for having AN as a major component. All the tested mixtures showed high retention ability ($\geq 98.9\%$) toward star anise and fennel EO (Figure S3). Figure 4 depicts the chromatogram of star anise EO obtained by SH-GC in presence of RAMEB:Lev and in presence of water as a reference solvent. Clearly, the peaks corresponding to the volatile compounds found in star anise are obvious in water but almost disappear in presence of the CD-based mixture. Figure S4 shows the chromatograms of star anise EO in the three other mixtures.

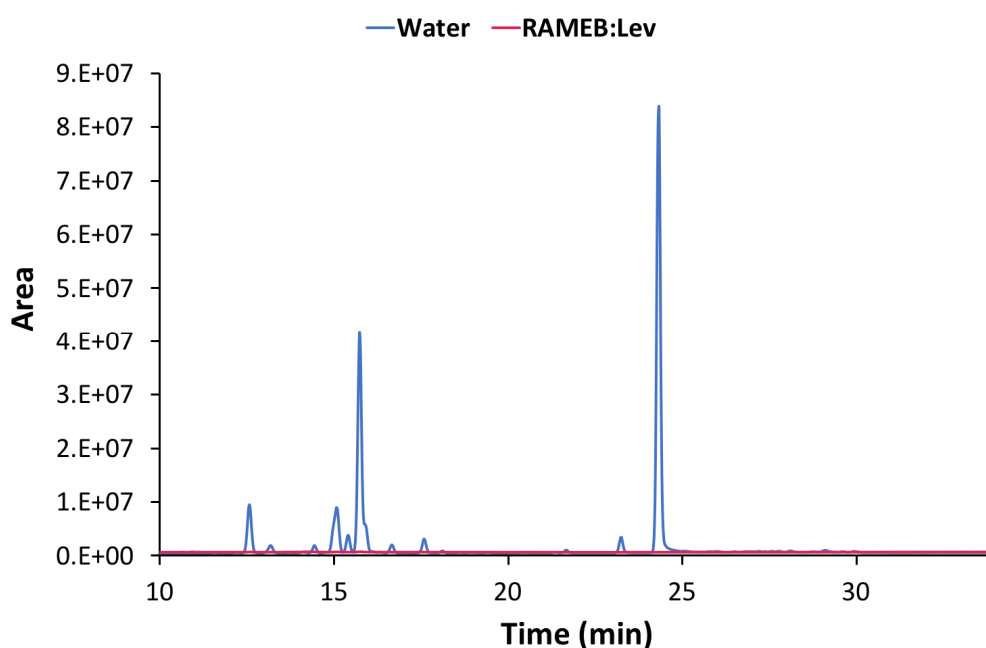


Figure 4. Chromatogram of star anise essential oil in water and in RAMEB:Lev.

Concerning the retention of AN, similar results were obtained regardless of whether AN was added in pure form or as a constituent of star anise or fennel EO (Figure S5). Therefore, the ability of the mixtures to retain AN was not affected by the simultaneous presence of other compounds.

3.5. Release study

Finally, the release of AN from the LMM was monitored by MHE. As described above, 10 successive headspace extractions were conducted at one-hour intervals. The amount of AN present in the vial after each extraction could be determined using the peak area. The retention ability of the LMM can be monitored and compared to water. The release profiles of AN from LMM and water are shown in Fig. 5. The results indicate that these CD-based mixtures can not only solubilize AN but also delay its release over time. Indeed, 70% of AN was released from water after 10 extractions at 60 °C, while only 20-40% was released from the CD:Lev mixtures.

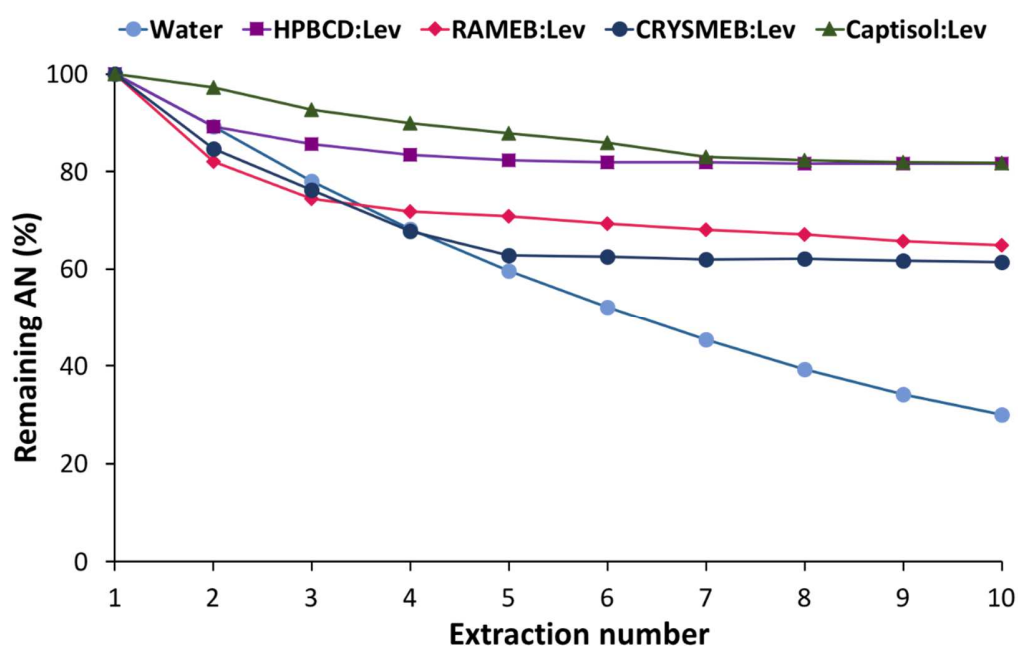


Figure 5. Release of *trans*-anethole from water and from supramolecular mixtures.

4. Conclusions

New supramolecular mixtures based on β -CD derivatives and levulinic acid were prepared, characterized and studied for their ability to solubilize AN and related essential oils. In addition, their thermal stability was investigated. The physicochemical characterization studies demonstrated that these CD-based mixtures are liquid at room temperature with relatively low viscosity. The stability studies also revealed that they were stable up to 60 °C and that no degradation could be detected after 18 months of storage. These mixtures also presented high solubilizing ability towards AN, star anise and fennel essential oils, when compared with water or aqueous solutions of CD. Furthermore, they were able to delay the release of AN, as shown by MHE experiments. When compared to aqueous CD solutions, these mixtures guarantee the presence of high amounts of CD associated to a liquid state over a wide temperature range, which consequently allow the broadening of CD applications. These mixtures may therefore contribute in the search for greener solvents and result in new promising, safe and economic drug delivery systems. Indeed, due to their peculiar properties (viscosity, stability and encapsulation properties), these supramolecular LMM could solubilize poorly water-soluble drugs and/or protect fragile molecules during topical cutaneous administration. The potential of these LMM is currently being tested for the treatment of cutaneous leishmaniasis with a volatile and poorly water-soluble anti leishmaniasis drug and the results will be communicated in due course.

Acknowledgements

The authors thank the Research Funding Program at the Lebanese University, Lebanon, and the Agence Universitaire de la Francophonie, Moyen-Orient (PCSI 2018-2020) for funding the project. Tracy El Achkar is grateful to the Université du Littoral Côte d'Opale and the Lebanese University for providing her a scholarship. Fanny SIMELIERE from Institut Galien Paris-Sud (Châtenay-Malabry, France) and Jacques LOUBENS from TA Instruments (Guyancourt, France) are greatly acknowledged for their generous help. This work partially benefited from the support of the project ParasiDES ANR-19-CE18-0027 of the French National Research Agency (ANR).

References

- Abbott, A.P., Capper, G., Davies, D.L., Rasheed, R.K., Tambyrajah, V., 2003. Novel solvent properties of choline chloride/urea mixtures. *Chem. Commun.* 70–71. <https://doi.org/10.1039/b210714g>
- Athanasiadis, V., Grigorakis, S., Lalas, S., Makris, D.P., 2018. Methyl β -cyclodextrin as a booster for the extraction for *Olea europaea* leaf polyphenols with a bio-based deep eutectic solvent. *Biomass Convers. Biorefinery* 8, 345–355. <https://doi.org/10.1007/s13399-017-0283-5>
- Auezova, L., Najjar, A., Kfoury, M., Fourmentin, S., Greige-Gerges, H., 2020. Antibacterial activity of free or encapsulated selected phenylpropanoids against *Escherichia coli* and *Staphylococcus epidermidis*. *J. Appl. Microbiol.* 128, 710–720. <https://doi.org/10.1111/jam.14516>
- Bakirtzi, C., Triantafyllidou, K., Makris, D.P., 2016. Novel lactic acid-based natural deep eutectic solvents: Efficiency in the ultrasound-assisted extraction of antioxidant polyphenols from common native Greek medicinal plants. *J. Appl. Res. Med. Aromat. Plants* 3, 120–127. <https://doi.org/10.1016/j.jarmap.2016.03.003>

453 Castro, V.I.B., Craveiro, R., Silva, J.M., Reis, R.L., Paiva, A., Duarte, A.R.C., 2018. Natural
 454 deep eutectic systems as alternative nontoxic cryoprotective agents. *Cryobiology* 83, 15–
 455 26. <https://doi.org/10.1016/j.cryobiol.2018.06.010>

456 Choi, Y.H., van Spronsen, J., Dai, Y., Verberne, M., Hollmann, F., Arends, I.W.C.E., Witkamp,
 457 G.-J., Verpoorte, R., 2011. Are natural deep eutectic solvents the missing link in
 458 understanding cellular metabolism and physiology? *Plant Physiol.* 156, 1701–1705.
 459 <https://doi.org/10.1104/pp.111.178426>

460 Ciobanu, A., Landy, D., Fourmentin, S., 2013. Complexation efficiency of cyclodextrins for
 461 volatile flavor compounds. *Food Res. Int.* 53, 110–114.
 462 <https://doi.org/10.1016/j.foodres.2013.03.048>

463 Crini, G., 2014. Review : A history of cyclodextrins. *Chem. Rev.* 114, 10940–10975.
 464 <https://doi.org/10.1021/cr500081p>

465 Crini, G., Fourmentin, S., Fenyvesi, É., Torri, G., Fourmentin, M., Morin-Crini, N., 2018.
 466 Cyclodextrins, from molecules to applications. *Environ. Chem. Lett.* 16, 1361–1375.
 467 <https://doi.org/10.1007/s10311-018-0763-2>

468 Dai, Y., van Spronsen, J., Witkamp, G.-J., Verpoorte, R., Choi, Y.H., 2013. Natural deep
 469 eutectic solvents as new potential media for green technology. *Anal. Chim. Acta* 766, 61–
 470 68. <https://doi.org/10.1016/j.aca.2012.12.019>

471 Decock, G., Landy, D., Surpateanu, G., Fourmentin, S., 2008. Study of the retention of aroma
 472 components by cyclodextrins by static headspace gas chromatography. *J. Incl. Phenom.*
 473 *Macrocycl. Chem.* 62, 297–302. <https://doi.org/10.1007/s10847-008-9471-z>

474 Delgado-Mellado, N., Larriba, M., Navarro, P., Rigual, V., Ayuso, M., García, J., Rodríguez, F.,
 475 2018. Thermal stability of choline chloride deep eutectic solvents by TGA/FTIR-ATR
 476 analysis. *J. Mol. Liq.* 260, 37–43. <https://doi.org/10.1016/j.molliq.2018.03.076>

477 Di Pietro, M.E., Dugoni, G.C., Ferro, M., Mannu, A., Castiglione, F., Gomes, M.C., Fourmentin,
 478 S., Mele, A., 2019. Do cyclodextrins encapsulate volatiles in deep eutectic systems? *ACS*

479 Sustain. Chem. Eng. 7, 17397–17405. <https://doi.org/10.1021/acssuschemeng.9b04526>

480 Diao, W.R., Hu, Q.P., Zhang, H., Xu, J.G., 2014. Chemical composition, antibacterial activity
481 and mechanism of action of essential oil from seeds of fennel (*Foeniculum vulgare* Mill.).
482 Food Control 35, 109–116. <https://doi.org/10.1016/j.foodcont.2013.06.056>

483 Dugoni, G.C., Di Pietro, M.E., Ferro, M., Castiglione, F., Ruellan, S., Moufawad, T., Moura, L.,
484 Gomes, M.F.C., Fourmentin, S., Mele, A., 2019. Effect of water on deep eutectic solvent/ β -
485 cyclodextrin systems. ACS Sustain. Chem. Eng. 7, 7277–7285.
486 <https://doi.org/10.1021/acssuschemeng.9b00315>

487 El Achkar, T., Fourmentin, S., Greige-gerges, H., 2019. Deep eutectic solvents : An overview on
488 their interactions with water and biochemical compounds. J. Mol. Liq. 288, 111028.
489 <https://doi.org/10.1016/j.molliq.2019.111028>

490 El Achkar, T., Moufawad, T., Ruellan, S., Landy, D., Greige-Gerges, H., Fourmentin, S., 2020.
491 Cyclodextrins: from solute to solvent. Chem. Commun. 56, 3385–3388.
492 <https://doi.org/10.1039/d0cc00460j>

493 Ferreira, M., Jérôme, F., Bricout, H., Manuel, S., Landy, D., Fourmentin, S., Tilloy, S., Monflier,
494 E., 2015. Rhodium catalyzed hydroformylation of 1-decene in low melting mixtures based
495 on various cyclodextrins and N,N'-dimethylurea. Catal. Commun. 63, 62–65.
496 <https://doi.org/10.1016/j.catcom.2014.11.001>

497 Fourmentin, S., Landy, D., Moura, L., Tilloy, S., Bricout, H., Ferreira, M., 2016. Procédé
498 d'épuration d'un effluent gazeux. FR3058905A1.

499 Francisco, M., van den Bruinhorst, A., Kroon, M.C., 2012. New natural and renewable low
500 transition temperature mixtures (LTTMs): screening as solvents for lignocellulosic biomass
501 processing. Green Chem. 14, 2153–2157. <https://doi.org/10.1039/c2gc35660k>

502 Imperato, G., Eibler, E., Niedermaier, J., König, B., 2005. Low-melting sugar-urea-salt mixtures
503 as solvents for Diels-Alder reactions. Chem. Commun. 1170–1172.
504 <https://doi.org/10.1039/b414515a>

505 Jeong, K.M., Jin, Y., Yoo, D.E., Han, S.Y., Kim, E.M., Lee, J., 2018. One-step sample
 506 preparation for convenient examination of volatile monoterpenes and phenolic compounds
 507 in peppermint leaves using deep eutectic solvents. *Food Chem.* 251, 69–76.
 508 <https://doi.org/10.1016/j.foodchem.2018.01.079>

509 Jérôme, F., Ferreira, M., Bricout, H., Menuel, S., Monflier, E., Tilloy, S., 2014. Low melting
 510 mixtures based on β -cyclodextrin derivatives and N,N'-dimethylurea as solvents for
 511 sustainable catalytic processes. *Green Chem.* 16, 3876–3880.
 512 <https://doi.org/10.1039/C4GC00591K>

513 Kfoury, M., Auezova, L., Greige-Gerges, H., Fourmentin, S., 2019. Encapsulation in
 514 cyclodextrins to widen the applications of essential oils. *Environ. Chem. Lett.* 17, 129–143.
 515 <https://doi.org/10.1007/s10311-018-0783-y>

516 Kfoury, M., Auezova, L., Greige-Gerges, H., Fourmentin, S., 2015. Promising applications of
 517 cyclodextrins in food: Improvement of essential oils retention, controlled release and
 518 antiradical activity. *Carbohydr. Polym.* 131, 264–272.
 519 <https://doi.org/10.1016/j.carbpol.2015.06.014>

520 Kfoury, M., Auezova, L., Greige-Gerges, H., Ruellan, S., Fourmentin, S., 2014a. Cyclodextrin,
 521 an efficient tool for trans-anethole encapsulation: chromatographic, spectroscopic, thermal
 522 and structural studies. *Food Chem.* 164, 454–61.
 523 <https://doi.org/10.1016/j.foodchem.2014.05.052>

524 Kfoury, M., Landy, D., Auezova, L., Greige-Gerges, H., Fourmentin, S., 2014b. Effect of
 525 cyclodextrin complexation on phenylpropanoids' solubility and antioxidant activity. *Beilstein*
 526 *J. Org. Chem.* 10, 2322–2331. <https://doi.org/10.3762/bjoc.10.241>

527 Kolb, B., Ettre, L.S., 2006. *Static Headspace–Gas Chromatography: Theory and Practice*. John
 528 Wiley & Sons, Inc., Hoboken, New Jersey.

529 Kurkov, S. V., Loftsson, T., 2013. Cyclodextrins. *Int. J. Pharm.* 453, 167–180.
 530 <https://doi.org/10.1016/j.ijpharm.2012.06.055>

531 Landy, D., Mallard, I., Ponchel, A., Monflier, E., Fourmentin, S., 2012. Remediation technologies
 532 using cyclodextrins: An overview. *Environ. Chem. Lett.* 10, 225–237.
 533 <https://doi.org/10.1007/s10311-011-0351-1>
 534 Legrand, F.X., Sauthier, M., Flahaut, C., Hachani, J., Elfakir, C., Fourmentin, S., Tilloy, S.,
 535 Monflier, E., 2009. Aqueous hydroformylation reaction mediated by randomly methylated
 536 beta-cyclodextrin: How substitution degree influences catalytic activity and selectivity. *J.*
 537 *Mol. Catal. A Chem.* 303, 72–77. [https://doi.org/DOI 10.1016/j.molcata.2008.12.017](https://doi.org/DOI%2010.1016/j.molcata.2008.12.017)
 538 Li, J.H., Li, W., Luo, S., Ma, C.H., Liu, S.X., 2019. Alternate ultrasound/microwave digestion for
 539 deep eutectic hydro-distillation extraction of essential oil and polysaccharide from
 540 *schisandra chinensis* (Turcz.) Baill. *Molecules* 24.
 541 <https://doi.org/10.3390/molecules24071288>
 542 Li, Z., Lee, P.I., 2016. Investigation on drug solubility enhancement using deep eutectic solvents
 543 and their derivatives. *Int. J. Pharm.* 505, 283–288.
 544 <https://doi.org/10.1016/j.ijpharm.2016.04.018>
 545 Loftsson, T., Masson, M., 2001. Cyclodextrins in topical drug formulations: theory and practice.
 546 *Int. J. Pharm.* 225, 15–30. [https://doi.org/10.1016/S0378-5173\(01\)00761-X](https://doi.org/10.1016/S0378-5173(01)00761-X)
 547 Marques, H.M.C., 2010. A review on cyclodextrin encapsulation of essential oils and volatiles.
 548 *Flavour Fragr. J.* 25, 313–326. <https://doi.org/10.1002/ffj.2019>
 549 Mbous, Y.P., Hayyan, M., Hayyan, A., Wong, W.F., Hashim, M.A., Looi, C.Y., 2017.
 550 Applications of deep eutectic solvents in biotechnology and bioengineering—Promises and
 551 challenges. *Biotechnol. Adv.* 35, 105–134. <https://doi.org/10.1016/j.biotechadv.2016.11.006>
 552 McCune, J.A., Kunz, S., Olesińska, M., Scherman, O.A., 2017. DESolution of CD and CB
 553 Macrocycles. *Chem. - A Eur. J.* 23, 8601–8604. <https://doi.org/10.1002/chem.201701275>
 554 Morrison, H.G., Sun, C.C., Neervannan, S., 2009. Characterization of thermal behavior of deep
 555 eutectic solvents and their potential as drug solubilization vehicles. *Int. J. Pharm.* 378, 136–
 556 139. <https://doi.org/10.1016/j.ijpharm.2009.05.039>

557 Moufawad, T., Moura, L.M., Ferreira, M., Bricout, H., Tilloy, S., Monflier, E., Gomes, M.C.,
 558 Landy, D., Fourmentin, S., 2019. First evidence of cyclodextrin inclusion complexes in a
 559 deep eutectic solvent. *ACS Sustain. Chem. Eng.* 7, 6345–6351.
 560 <https://doi.org/10.1021/acssuschemeng.9b00044>

561 Moura, L., Moufawad, T., Ferreira, M., Bricout, H., Tilloy, S., Monflier, E., Costa Gomes, M.F.,
 562 Landy, D., Fourmentin, S., 2017. Deep eutectic solvents as green absorbents of volatile
 563 organic pollutants. *Environ. Chem. Lett.* 747–753. [https://doi.org/10.1007/s10311-017-](https://doi.org/10.1007/s10311-017-0654-y)
 564 0654-y

565 Nguyễn, C.H., Putaux, J.-L., Santoni, G., Tfaïli, S., Fourmentin, S., Coty, J.-B., Choïnard, L.,
 566 Gèze, A., Wouessidjewe, D., Barratt, G., Lesieur, S., Legrand, F.-X., 2017. New
 567 nanoparticles obtained by co-assembly of amphiphilic cyclodextrins and nonlamellar single-
 568 chain lipids: Preparation and characterization. *Int. J. Pharm.* 531, 444–456.
 569 <https://doi.org/10.1016/j.ijpharm.2017.07.007>

570 Ozturk, B., Esteban, J., Gonzalez-Miquel, M., 2018. Deterpenation of citrus essential oils using
 571 glycerol-based deep eutectic solvents. *J. Chem. Eng. Data* 63, 2384–2393.
 572 <https://doi.org/10.1021/acs.jced.7b00944>

573 Potier, J., Menuel, S., Fournier, D., Fourmentin, S., Woisel, P., Monflier, E., Hapiot, F., 2012.
 574 Cooperativity in aqueous organometallic catalysis: Contribution of cyclodextrin-substituted
 575 polymers. *ACS Catal.* 2, 1417–1420. <https://doi.org/10.1021/cs300254t>

576 Rodriguez Rodriguez, N., Van Den Bruinhorst, A., Kollau, L.J.B.M., Kroon, M.C., Binnemans, K.,
 577 2019. Degradation of deep-eutectic solvents based on choline chloride and carboxylic
 578 acids. *ACS Sustain. Chem. Eng.* 7, 11521–11528.
 579 <https://doi.org/10.1021/acssuschemeng.9b01378>

580 Szejtli, J., 1998. Introduction and general overview of cyclodextrin chemistry. *Chem. Rev.* 98,
 581 1743–1753. <https://doi.org/10.1021/CR970022C>

582 Tabary, N., Mahieu, A., Willart, J.F., Dudognon, E., Dande, F., Descamps, M., Bacquet, M.,

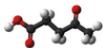
583 Martel, B., 2011. Characterization of the hidden glass transition of amorphous
 584 cyclomaltoheptaose. *Carbohydr. Res.* 346, 2193–2199.
 585 <https://doi.org/10.1016/j.carres.2011.07.010>
 586 Tang, B., Row, K.H., 2013. Recent developments in deep eutectic solvents in chemical
 587 sciences. *Monatshefte für Chemie - Chem. Mon.* 144, 1427–1454.
 588 <https://doi.org/10.1007/s00706-013-1050-3>
 589 Triolo, A., Lo Celso, F., Russina, O., 2020. Structural features of β -cyclodextrin solvation in the
 590 deep eutectic solvent, *reline*. *J. Phys. Chem. B* 124, 2652–2660.
 591 <https://doi.org/10.1021/acs.jpcb.0c00876>
 592 Wang, B., Zhang, G., Yang, M., Liu, N., Li, Y.X., Ma, H., Ma, L., Sun, T., Tan, H., Yu, J., 2018.
 593 Neuroprotective effect of anethole against neuropathic pain induced by chronic constriction
 594 injury of the sciatic nerve in mice. *Neurochem. Res.* 43, 2404–2422.
 595 <https://doi.org/10.1007/s11064-018-2668-7>
 596 Zhang, Q., De Oliveira Vigier, K., Royer, S., Jérôme, F., 2012. Deep eutectic solvents:
 597 syntheses, properties and applications. *Chem. Soc. Rev.* 41, 7108–7146.
 598 <https://doi.org/10.1039/c2cs35178a>
 599

Modified β -cyclodextrins

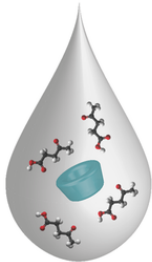


mp > 280 °C

+

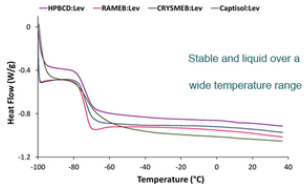


Levulinic acid



New liquid mixtures
based on cyclodextrins

Physicochemical
characterization



Solubilization of
bioactive compounds

